ISSN 1392 - 1207. MECHANIKA. 2009. Nr.4(78)

Dependence of ultimate tensile strength of friction stir welded AA2024-T6 aluminium alloy on friction stir welding process parameters

N. Shanmuga Sundaram*, N. Murugan**
**Department of Mechanical Engineering, PSG College of Technology, Coimbatore, India - 641004,*
E-mail: nss.mechanical@gmail.com
***Department of Mechanical Engineering, Coimbatore Institute of Technology, Coimbatore, India - 641014,*
E-mail: drnmurugan@gmail.com

1. Introduction

Friction stir welding (FSW) is a relatively new joining technique developed by TWI, Cambridge, in 1991 [1]. This new technology can join aluminium alloys that are difficult to weld by traditional fusion techniques, for example alloys belonging to the 2xxx series with limited weldability [2]. Conventional welding of these alloys results in a dendritic structure in the fusion zone which leads to a drastic decrease of the mechanical properties [3]. As FSW is a solid state process the solidification structure is absent in the weld and the problem related to the presence of brittle dendritic and eutectic phases is eliminated [4]. In addition, the surface oxide is not deterrent for the process and no particular cleaning operations are needed prior to welding.

Among the 2xxx series aluminium alloy 2024 is extensively used in the aircraft industry for applications such as fuselage skins, fuselage frames, and wings due to its high strength to weight ratio and high fracture toughness [5]. Friction stir welding of AA 2024 and their characterization were reported by various authors. Hakan Aydin et al [6] pointed out the presence of a hardness degradation region (i.e. softened region), composed of weld nugget (WN), thermo mechanically affected zone (TMAZ) and heat affected zone (HAZ) and thus the tensile properties of the FSW joints were lower than those of the base materials.

The predominant factors which have greater influence on tensile strength of friction stir welded aluminium alloys were identified as tool pin profiles, tool rotational speed, welding speed and tool axial downward force [7]. Friction stir welded joints were successfully made using various tool pin profiles and their characterization was reported by various authors. Elangovan et al [8] studied the effect of five different pin profiles viz. straight cylindrical, tapered cylindrical, threaded cylindrical, triangular and square, on friction stir processing zone of AA6061 aluminium alloy. Tensile properties of the FSW joints were evaluated, and it was reported that the square tool pin profile produces joints with higher strength and defect free welds compared to other tool pin profiles.

In most of the reported research works on FS welding of AA 2024, it is observed that the interaction effect of FSW process parameters on tensile strength of FS welded AA 2024-T6 is not studied. The present research was done with a newly designed hexagonal cross-section pinned tool with three different diameters. Since the tool pin diameter mainly determines the width of weld nugget (WN) and heat affected zone (HAZ), it is introduced as a new process parameter along with other three process parameters. The present research work is aimed to evaluate the interaction effects of four process parameters viz., tool rotational speed N, welding speed S, tool pin diameter D and tool axial plunging force F on the tensile strength of FS welded AA2024 -T6 joints fabricated using the newly developed tool. Response surface method (RSM) was employed to develop the regression model, to correlate the FSW process parameters with tensile strength and to evaluate the interaction effects.

2. Experimental procedures

The experimental set up consists of a special purpose machine having dedicated arrangements designed for the friction stir welding. Fig. 1 shows the friction stir welding machine and the AA 2024-T6 work pieces fitted with the fixtures of the machine.

a

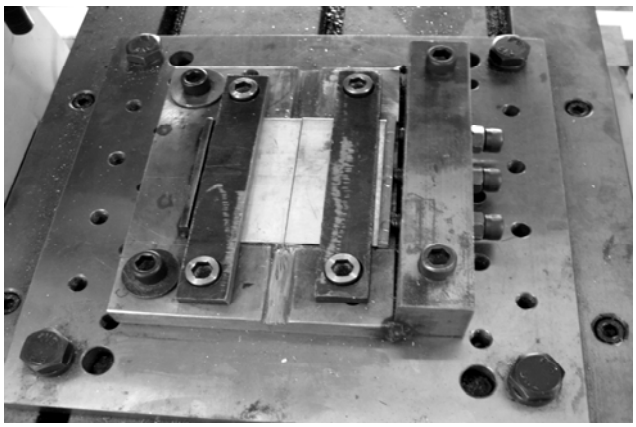

b

Fig. 1 Friction stir welding machine: a - photograph of the machine, b - photograph showing the work pieces fitted on the table with specially designed fixtures

The vertical tool head can be moved along the vertical guide ways (Z axis). The horizontal table can be moved along X and Y axis and consists of mechanical fixtures to hold the work pieces rigidly. The machine can be operated in wide range of tool rotational speed, welding speed and tool axial force.

Three different tools made of HSS having different pin diameter and with hexagonal profile were used to fabricate the FSW joints. The reason behind in designing the hexagonal profiled pin was the six sides of the pin would create higher friction and good material flow between the plates, compared to the smooth cylindrical and threaded profiles. The profile and dimensions of the tools are shown in Fig. 2.

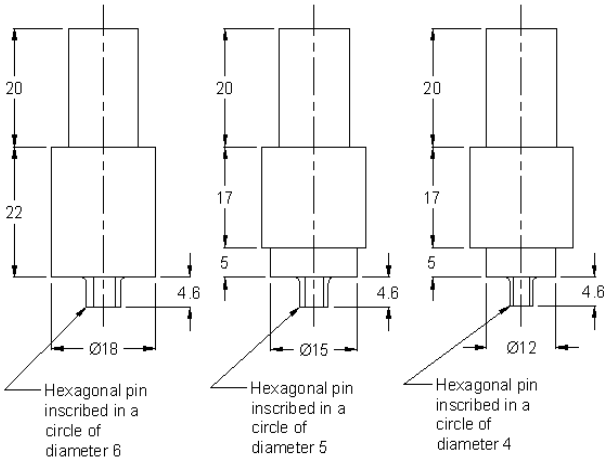

a

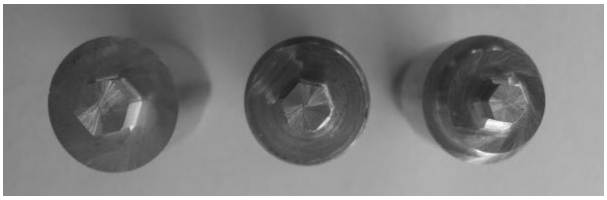

b

Fig. 2 Friction stir welding tools: a - profile and dimensions of the tools, b - photograph of the FSW tools

Aluminium alloy AA2024-T6 is heat treatable and T6 denotes solution heat treated and artificially aged. The chemical composition and mechanical properties of the AA 2024-T6 aluminium alloy are given in Table 1 and 2. Aluminium rolled plates of 5 mm thickness cut into the required size of 100 mm x 50 mm were tightly secured by mechanical clamping. The longitudinal direction of the FSW was perpendicular to the rolling direction of 2024 aluminium alloy. Single pass butt welding procedure was followed to fabricate the joints. The tool was rotated in the clockwise direction, while the specimens fixed on the table were moved from left side to right side. The side in which both the direction of tool rotation and the direction of welding are the same is termed as advancing side; and the other side they are opposite in direction is termed as retreating side [9].

Trial experiments were conducted to find the working range of the operating parameters viz. tool rotational speed *N*, welding speed *S* and tool axial plunging force *F*. Feasible limits of the parameter were decided based on visual inspection for the smooth appearance without any visual defects such as cracks, under cut, etc. Typical defective and defect free friction stir welds are shown in Fig. 3. These defects were due to the material splash at higher rotational speed instead of plastic deformation. The operating parameters and their working range for FSW of AA 2024-T6 are tabulated in Table 3.

Four factors, three levels Box-Behnken experimental design shown in Table 4, was selected for conducting the experiments. The Aluminium plates were FS welded as per the design matrix. Two tensile specimens from each welded plate were prepared as per the American Society for Testing of Materials (ASTM E8M-04) standards. The photographs of typical fabricated tensile testing specimens are shown in Fig. 4. The Ultimate Tensile Strength (UTS) of the FS welded joints were evaluated in Universal Testing Machine (make - ALFRED J. Amsler & Co, Switzerland). The average values of UTS of the tensile specimens and joint efficiency were calculated and presented in Table 4.

Table 1

Chemical composition of the base metal AA 2024-T6

Al	Cu	Mg	Mn	Si	Fe	Zn	Cr	Ni	Ti
93.35 %	4.424 %	1.315 %	0.522 %	0.09 %	0.116 %	0.041 %	0.005 %	0.005 %	0.013 %

Table 2

Mechanical properties of the base metal AA 2024-T6

Yield strength, MPa	Ultimate Tensile Strength (UTS), MPa	Percentage of elongation, %	Micro hardness (VHN)
382.0	410.0	20.0	185.0

Table 3

FSW operating parameters and their levels selected

S. No.	Operating Parameter	Symbol	Unit	Levels		
				-1	0	1
1	Tool rotational speed	*N*	rpm	500	900	1300
2	Welding speed	*S*	mm/min	30	50	70
3	Tool pin diameter	*D*	mm	4	5	6
4	Tool axial plunging force	*F*	kN	14.72	24.53	34.33

Table 4

Design matrix with its experimental results and predicted model value

Trial run	FSW process parameters				σ_{ut}, MPa		Error	Joint efficiency*
	N	*S*	*D*	*F*	Esti-mated	Pre-dicted	%	%
1	-1	-1	0	0	288.5	289.1	-0.2	70.4
2	+1	-1	0	0	245.7	253.2	-3.0	59.9
3	-1	+1	0	0	243.8	241.2	1.1	59.5
4	+1	+1	0	0	295.2	299.4	-1.4	72.0
5	0	0	-1	-1	287.3	287.3	0.0	70.1
6	0	0	+1	-1	295.4	295.9	-0.2	72.0
7	0	0	-1	+1	291.5	295.9	-1.5	71.1
8	0	0	+1	+1	282.3	287.2	-1.7	68.9
9	-1	0	0	-1	250.8	253.2	-0.9	61.2
10	+1	0	0	-1	300.9	301.1	-0.1	73.4
11	-1	0	0	+1	284.5	289.9	-1.9	69.4
12	+1	0	0	+1	261.1	264.3	-1.2	63.7
13	0	-1	-1	0	291.8	295.7	-1.3	71.2
14	0	+1	-1	0	269.3	274.7	-2.0	65.7
15	0	-1	+1	0	275.4	275.6	-0.1	67.2
16	0	+1	+1	0	293.1	294.8	-0.6	71.5
17	-1	0	-1	0	275.9	271.5	1.6	67.3
18	+1	0	-1	0	292.4	283.3	3.2	71.3
19	-1	0	+1	0	273.5	272.2	0.5	66.7
20	+1	0	+1	0	288.6	282.6	2.1	70.4
21	0	-1	0	-1	285.7	283.3	0.8	69.7
22	0	+1	0	-1	287.2	286.5	0.2	70.0
23	0	-1	0	+1	297.1	287.3	3.4	72.5
24	0	+1	0	+1	290.5	282.4	2.9	70.9
25	0	0	0	0	305.3	310.3	-1.6	74.5
26	0	0	0	0	310.8	310.3	0.2	75.8
27	0	0	0	0	314.9	310.3	1.5	76.8

UTS - Ultimate Tensile Strength * - Based on Experimental UTS

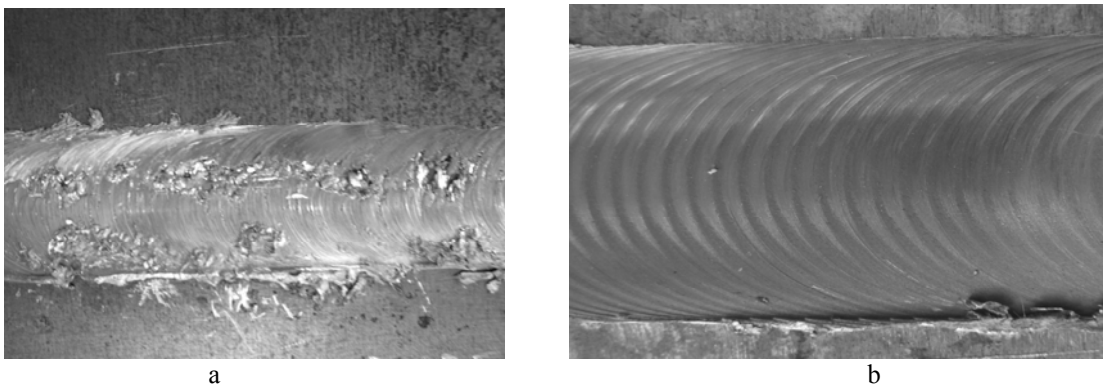

a b

Fig. 3 Appearance of friction stir weld: a - typical defective friction stir weld (N = 1900 rpm, S = 120 mm/min, D = 5 mm and F = 34.33 kN), b - close view of typical defective free friction stir weld (N = 1300 rpm, S = 70 mm/min, D = 5 mm and F = 24.53 kN)

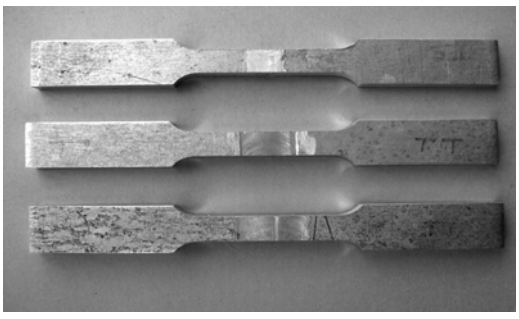

Fig. 4 Photograph of typical tensile specimens fabricated with three different diameter pinned tool

3. Developing mathematical models

The response function representing the ultimate tensile strength σ_{ut}, of the FS welded joint is a function of tool rotational speed N, welding speed S, tool pin diameter D and tool axial plunging force F and can be expressed as

$$UTS = f(N, S, D, F) \quad (1)$$

The second order polynomial (regression) equation used to represent the response surface 'Y' for K factors is given by

$$Y = b_0 + \sum b_i x_i + \sum b_{ii} x_i^2 + \sum b_{ij} x_i x_j \quad (2)$$

Where b_0 is the average of responses and b_i , b_{ii} and b_{ij} are the coefficients that depend on respective main and interaction effects of the parameters. The values of the coefficients are calculated using the following expressions [10, 11].

$$b_0 = 0.142857 (\sum Y) - 0.035714 \sum \sum (X_{ii} Y) \quad (3)$$

$$b_i = 0.041667 \sum (X_i Y) \quad (4)$$

$$b_{ii} = 0.03125 \sum (X_{ii} Y) + 0.00372 \sum \sum (X_{ii} Y) - 0.035714 (\sum Y) \quad (5)$$

$$b_{ij} = 0.0625 \sum (X_{ij} Y) \quad (6)$$

For four factors the selected polynomial could be expressed as

$$UTS = b_0 + b_1 (N) + b_2 (S) + b_3 (D) + b_4 (F) + b_{11} (N^2) + b_{22} (S^2) + b_{33} (D^2) + b_{44} (F^2) + b_{12} (NS) + b_{13} (ND) + b_{14} (NF) + b_{23} (SD) + b_{24} (SF) + b_{34} (DF) \quad (7)$$

The coefficients of the polynomial equation were determined using statistical software SYSTAT-version 12. The mathematical model in coded form to predict the ultimate tensile strength of the FS welded AA2024-T6 is given by

$$UTS = 310.3 + 5.575\,N - 0.425\,S + 0.008\,D - 0.025\,F - 23.7\,N^2 - 15.9\,S^2 - 9.25\,D^2 - 9.525\,F^2 + 23.55\,NS - 0.35\,ND - 18.38\,NF + 10.05\,SD - 2.025\,SF - 4.325\,DF \quad (8)$$

The predicted tensile strength from the model and its deviation from experimental values for the 27 runs are also tabulated in Table 4. The error in the predicted model value was calculated and found that it is within ± 6%.

Joint efficiency is calculated as the ratio between the tensile strength of the FS welded joint and the base metal. It is found that the joint efficiency varies between 55 and 75% and it is tabulated in Table 4.

4. Validation of the developed model

The developed model was tested by analysis of variance (ANOVA) using the statistical software SYSTAT-12 and the results are tabulated in Table 5. The value of R^2= 0.932 indicates that the model explains 93.2% of the total variability. Scatter plot of experimental value *Vs* predicted value plotted in Fig. 5 shows that the values are normally distributed. To test the accuracy of the model in actual applications, conformity test runs were conducted by assigning different values for process variables within their working limit but different from that of design matrix. These results indicated that the developed model best fits to find the UTS of FS welded AA2024-T6 aluminium alloy.

Table 5

ANOVA results of the model

Sum of squares	df	Mean square	*F*-ratio	Multiple *R*	Squared multiple *R*	Adjusted squared multiple *R*
7822.63	14	558.76	11.78	0.965	0.932	0.853

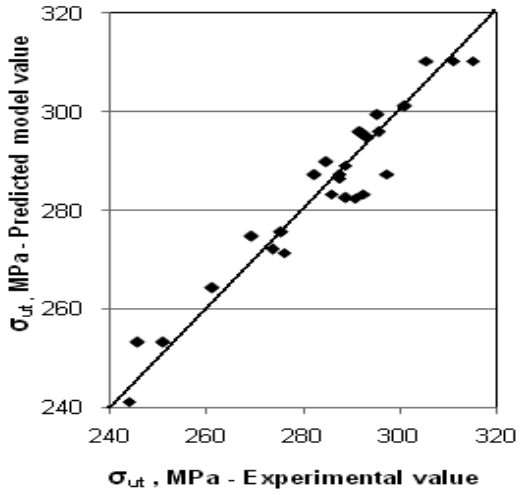

Fig. 5 Scatter plot of UTS

5. Results and discussions

The developed mathematical model was used to predict the ultimate tensile strength of the FS welded aluminium alloy AA2024-T6 with various combination of parameters. The predicted values were presented to analyze the interaction effect of various process parameters on tensile strength. It is found from the results that the ultimate tensile strength of FS welded joints was lower than the base metal irrespective of the operating parameters used to fabricate the joints. The four operating parameters considered are directly affecting the magnitude of frictional heat generated and extend of plastic flow of material [8]. In general, it is observed that when the combinations of parameters create very low / very high frictional heat and material flow then lower tensile strength was observed. Percentage of elongation of the FS welded joints varies between 8 and 15% and it shows that ductile fracture occurred during tensile testing.

5.1. Interaction effect of tool rotational speed *N* and welding speed *S* on UTS

Fig. 6 reveals the interaction effect of tool rotational speed and welding speed on tensile strength. UTS of FS welded joints increases with decrease in the welding

speed when the tool rotational speed is at 500 rpm, because of increase in the heat input. The tensile strength decreases with decrease in the welding speed when the tool rotational speed is at 1300 rpm which is due to the high temperature experienced by the materials [12, 13]. It is evident from the figure that higher σ_{ut} is observed when the welding speed is at 50 mm/min. σ_{ut} increases gradually to a maximum value when rotational speed increases up to 900 rpm and then decreases with further increase in N. Joints fabricated with the welding speed of 50 mm/min are observed with the highest tensile strength at the tool rotational speed of 900 rpm.

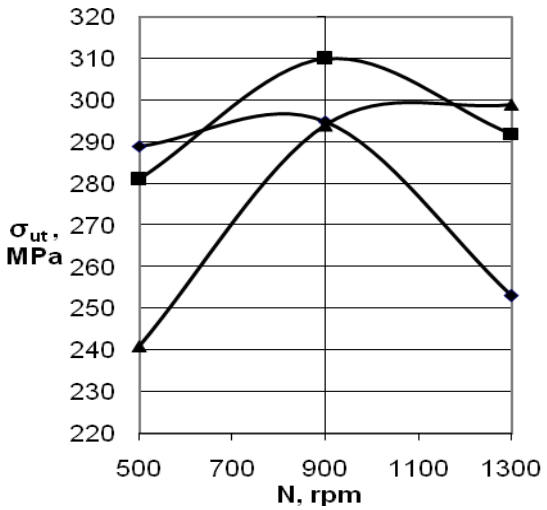

Fig. 6 Interaction effect of tool rotational speed N and welding speed (S = 30 mm/min (—◆—); S = 50 mm/min (—■—); S = 70 mm/min (—▲—)) on UTS σ_{ut}, when D = 5 mm, F = 24.53 kN

5.2. Effect of tool rotational speed N and tool pin diameter D on UTS

The effect of tool rotational speed and tool pin diameter is shown in Fig. 7. The diameter of the tool pin determines the width of the weld nugget and HAZ which affects the tensile strength of the FS welded joints. Tensile strength increases with increase in tool rotational speed up to 900 rpm and it decreases with further increase in rotational speed, irrespective of the tool pin diameter. Joints fabricated with intermediate tool pin diameter of 5 mm have higher tensile strength at all the three tool rotational speeds of 500 rpm, 900 rpm and 1300 rpm. Joints made with the pin diameter of 4 mm do not create the sufficient plastic flow of material and lower tensile strength is observed. On the other hand joints made with 6 mm diameter pin create higher turbulence and material flows out from the weld nugget and that results in lower tensile strength.

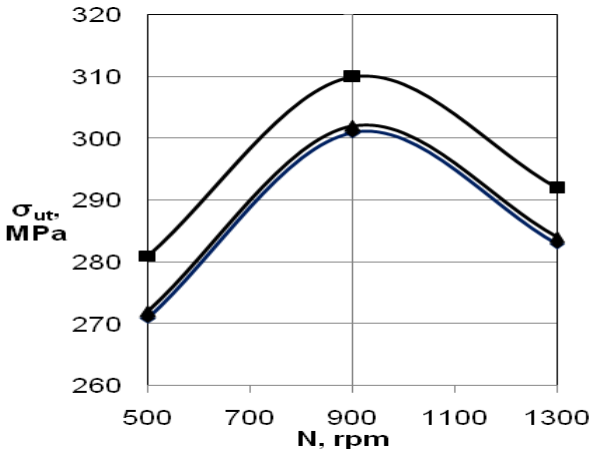

Fig. 7 Effect of tool rotational speed N at various tool pin diameters (D = 4 mm (—◆—); D = 5 mm (—■—); D = 6 mm (—▲—)) on UTS σ_{ut}, when S = 50 mm/min, F = 24.53 kN

5.3. Interaction effect of tool rotational speed N and tool axial force F on UTS

The interaction effect of tool rotational speed and tool axial plunging force is represented in Fig. 8. Oyuang and Kovacevic [14] observed that the axial force is directly responsible for the plunge depth of the tool into the work piece and load characteristics associated with linear friction stir weld. Tensile strength increases with increase in tool axial force when the tool rotational speed is at 500 rpm, because of increased friction between the tool and the work pieces. But when N is 1300 rpm, tensile strength decreases with increase in axial force which is due to the higher plunge depth of the tool that leads to the material over flow from the weld nugget. Tensile strength increases with increase in tool rotational speed up to 900 rpm and then decreases with increase in the rotational speed, when the tool axial force is at 24.5 kN. The highest tensile strength is observed when the tool rotational speed and axial force are at 900 rpm and 24.5 kN respectively.

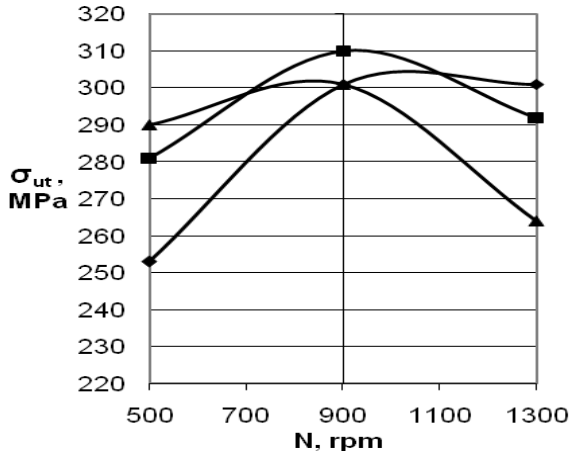

Fig. 8 Interaction effect of tool rotational speed N and tool axial force (F = 14.7 kN (—◆—); F = 24.5 kN (—■—); F = 34.3 kN (—▲—)) on UTS σ_{ut}, when S = 50 mm/min, D = 5 mm

5.4. Interaction effect of welding speed S and tool pin diameter D on UTS

Higher welding speed results in higher production rate. The softened area becomes narrower when the welding speed is higher. Thus, the tensile strength of FS welded aluminium alloy has direct relationship with welding speed [7]. Higher welding speeds are associated with low heat inputs, and faster cooling rates of the welded joint. This can significantly reduce the extent of metallurgical transformations taking place during welding (such as solubilisation, re-precipitation and coarsening of precipitates) and hence the local strength of individual regions across the

weld zone [12, 15]. Fig. 9 shows the interaction effect of welding speed and tool pin diameter on tensile strength of the FS welded joints. Tensile strength decreases with increase in tool pin diameter when the welding speed is at 30 mm/min which is due to the severe stirring that results in re-precipitation and coarsening of precipitates [12, 15]. When the welding speed is 70 mm/min, tensile strength increases with increase in tool pin diameter because of increased heat generated. Tensile strength increases with welding speed up to 50 mm/min and then decreases with further increases in the welding speed, when the tool pin diameter is 5 mm. When S is 50 mm/min highest tensile strength is observed with the tool pin diameter of 5 mm.

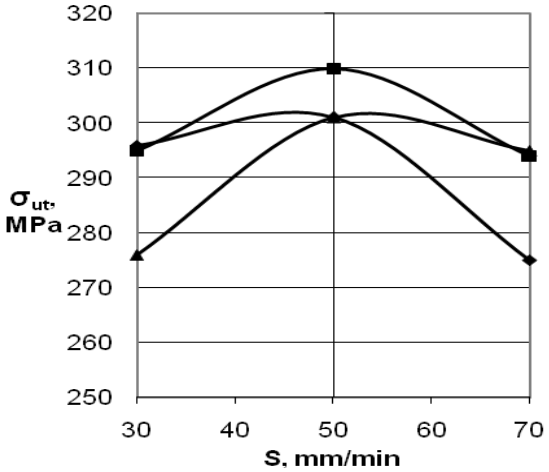

Fig. 9 Interaction effect of welding speed S and tool pin diameter (D = 4 mm (—◆—); D = 5 mm (—■—); D = 6 mm (—▲—)) on UTS σ_{ut}, when N = 900 rpm, F = 24.5 kN

5.5. Interaction effect of welding speed S and tool axial force F on UTS

The welding speed determines the softening of base metal where as the tool axial force determines the degree of friction between the tool and the work pieces. The interaction effect of welding speed and tool axial force is represented in Fig. 10; and it is evident that tensile strength increases with increase in welding speed up to 50 mm/min and then decreases with increase in welding speed, irrespective of the level of axial force. Joints made with an axial force of 14.7 kN and 24.5 kN have lower and higher tensile strength respectively when the welding speed is 30 mm/min. The lower and higher tensile strength of the joints are observed with the axial forces 34.3 kN and 24.5 kN, when the welding speed is at 70 mm/min. Joints made with the lowest axial force of 14.7 kN do not create sufficient friction between the tool and the work pieces, where as the joints made with the highest axial force of 34.3 kN have higher plunge depth of the tool and both resulted in lower tensile strength at all the three welding speeds considered. Joints made with an axial force of 24.5 kN have higher tensile strength at all the three welding speeds. The highest tensile strength is observed with an axial force of 24.5 kN and when the welding speed is at 50 mm/min.

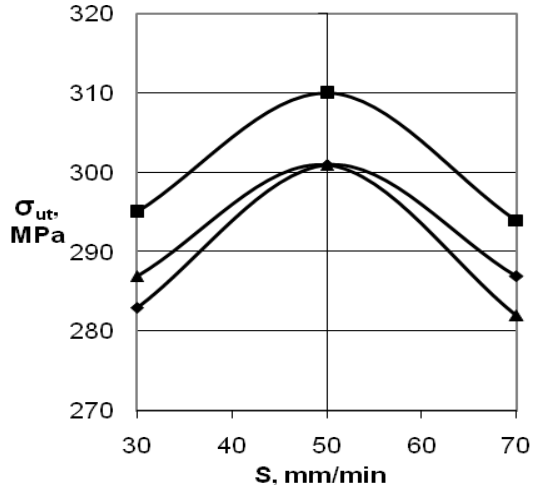

Fig. 10 Interaction effect of welding speed S and tool axial force (F = 14.7 kN (—◆—); F = 24.5 kN (—■—); F = 34.3 kN (—▲—)) on UTS σ_{ut}, when N = 900 rpm, D = 5 mm

5.6. Interaction effect of tool axial force F and tool pin diameter D on UTS

The heat input and temperature distribution during friction stir welding is due to the frictional heat generated between the rotating tool and surface of the plate to be welded and in turn depends on coefficient of friction. Apart from the properties of tool and plate material, the axial force decides the coefficient of friction. Hence axial force plays a significant role in friction stir welding process. The degree of material mixing and inter diffusion, the thickness of deformed aluminum lamellae, the material flow patterns highly depend on welding temperature, flow stress and axial force [16]. It is clear from the Fig. 11, that tensile strength increases with increase in axial force up to 24.5 kN and then decreases with further increases in axial force. At an axial force of 14.7 kN, the higher and lower tensile strength of the joints are observed with the tool pin diameters of 5 mm and 4 mm respectively. The higher and lower tensile strengths were obtained with the tool pin diameter of 5 mm and 6 mm respectively, when the axial force is 34.3 kN. Joints made with 5 mm diameter pinned tool have higher tensile strength at all the three axial forces

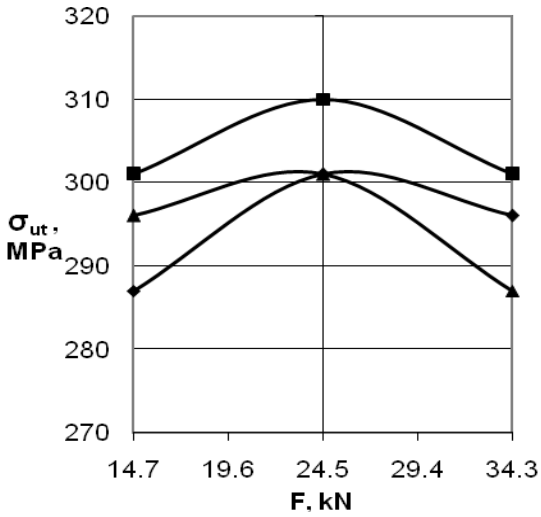

Fig. 11 Interaction effect of tool pin diameter D and tool axial force (F = 14.7 kN (—◆—); F = 24.5 kN (—■—); F = 34.3 kN (—▲—)) on UTS σ_{ut}, when N = 900 rpm, S = 50 mm/min

considered, which is due to the smooth material flow and sufficient frictional heat generated. The highest tensile strength is observed when the axial force of 24.5 kN and the tool pin diameter of 5 mm.

6. Conclusions

1. Aluminium alloy AA2024-T6 was successfully friction stir welded using the newly developed HSS tool and regression model to predict the tensile strength of the FS welded joints was developed and validated.

2. The developed model can be used to predict the tensile strength of the FS welded AA2024-T6 Aluminium alloy joints within ± 6% deviation.

3. Friction stir welded joints made within the operating window are free from defects and posses higher tensile strength. Tensile strength of the friction stir welded joints varies between 55 and 75% of the base metal strength. It is found to be good compared to the poor quality of weld produced by conventional fusion welding processes.

4. Most of the friction welded joints are failed by means of ductile fracture during tensile testing, and it is found from the percentage of elongation which varies between 8 and 15%.

5. The interaction effect of operating parameters viz. Tool rotational speed *N*, welding speed *S*, tool pin diameter *D*, tool axial force *F* are found to be significant. Increase in welding speed with increase in tool rotational speed within their operating range produce higher tensile strength joints. *N* between 700 rpm and 1100 rpm and *S* between 30 mm/min and 70 mm/min, produce FS welded joints with σ_{ut} more than 67% of the base metal.

6. Increase in rotational speed with decrease in axial force within their operating range tends to lower the tool plunge depth and consequently higher tensile strength of the joints. *N* between 700 rpm and 1100 rpm and *F* between 14.7 kN and 34.3 kN, produce FS welded joints with σ_{ut} more than 69% of the base metal.

7. Most of the joints fabricated with smallest and largest diameter pinned tool exhibited lower tensile strength. Joints fabricated with 5 mm diameter pinned tool have the highest tensile strength. FS welded joints fabricated using 5 mm diameter pinned tool with *N* between 700 rpm and 1100 rpm, produce σ_{ut} more than 73 % of the base metal.

7. In general, it is observed that when the combinations of parameters create very low / very high frictional heat and material flow then lower tensile strength was observed.

8. Friction stir welded aluminium alloy AA2024-T6 joints made with 5 mm diameter pinned tool; *N* between 700 rpm and 1100 rpm; *S* between 30 mm/min and 70 mm/min and *F* between 19.6 kN and 29.4 kN are found to be possessed more than 70% of the base metal tensile strength.

Acknowledgement

Friction Stir Welding of the work pieces and its Characterizations were performed at Welding Research Cell, Department of Mechanical Engineering, Coimbatore Institute of Technology, Coimbatore, India. The authors are grateful to all the staff members of Welding Research Cell. The authors would like to thank DRDO- Naval Research Board, INDIA, for providing financial support to procure the FSW machine for Welding Research Cell, CIT, Coimbatore.

References

1. **Thomas, W.M., Nicholas, E.D., Needham, J.C., Murch, M.G., Temple-Smith, P., Dawes, C.J.** Friction Stir Butt Welding. 1991, International Patent No.PCT/GB92/02203.
2. **Cavaliere, P., Cerri, E., Squillace, A.** Mechanical response of 2024-7075 aluminium alloys joined by friction stir welding.-Journal of Materials Science, 2005, 40, p.3669-3676.
3. **Su, J.Q., Nelson, T.W., Mishra, R., Mahoney, M.** Microstructural investigation of friction stir welded 7050-T651 aluminium.-Acta Materialia, 2003, p.51-713.
4. **Rhodes, C.G., Mahoney, M.W., Bingel, W.H.** Effect of friction stir welding on microstructure of 7075 aluminium.-Scripta Materilaia, 1997, 36, p.69-75.
5. **Starke, E.A., Jr., Staley, J.T.** Application of modern aluminum alloys to aircraft.-Progress in Aerospace Sciences, 1996, 32(2-3), p.131-172.
6. **Hakan Aydin, Ali Bayram, Agah Uguz, Kemal Setran Akay.** Tensile properties of friction stir welded joints of 2024 aluminium alloys in different heat-treated-state.-Journal of Materials and Design, 2009, 30, p.2211-2221.
7. **Won Bae Lee, Yun-Mo Yeon, Seung-Boo Jung** Mechanical properties related to micro structural variation of 6061 Al alloy joints by friction stir welding. -Materials Transactions, 2004, 45(5), p.1700-1705.
8. **Elangovan, K., Balasubramanian, V., Valliappan, M.** Influences of tool pin profile and axial force on the formation of friction stir processing zone in AA6061 aluminium alloy.-International Journal of Advanced Manufacturing Technology, 2008, 38, p.285-295.
9. **Scialpi A., De Filippis L.A.C., Cavaliere P.** Influence of shoulder geometry on microstructure and mechanical properties of friction stir welded 6082 aluminium alloy. -Materials and Design, 2007, 28, p.1124-1129.
10. **Gunaraj, V., Murugan, N.** Application of response surface methodology for predicting weld bead quality in submerged arc welding of pipes.-Journal of Material Processing Technology, 1999, 88, p.266-275.
11. **Manonmani, K., Murugan, N., Bhuvanasekaran, G.** Effect of process parameters on the weld bead geometry of laser beam welded stainless steel sheets. -International Journal of Joining of Materials, 2005, 17/4, p.103-109.
12. **Sunggon Lim., Sangshik Kim., Chang-Gil Lee., Sungjoon Kim.** Tensile behavior of Friction-Stir-Welded Al 6061-T651.-Metallurgical and Materials Transactions A, September 2004, 35A, p.2829-2835.
13. **Elangovan, K., Balasubramanian, V., Valliappan, M.** Effect of pin profile and rotational speed of the tool on the formation of friction stir processing zone in AA6061 aluminium alloy.-The International Journal of Advanced Manufacturing Technology, 2008, 38/3-4.
14. **Ouyang, JH., Kovacevic, R.** Material flow and microstructure of the friction stir butt welds of the same and

dissimilar aluminum alloys.-Journal of Materials Engineering and Performance, 2002, 11(1), p.51-63.
15. **Lomolino, S., Tovo, R., Dos Santos, J.** On the fatigue behavior and design curves of friction stir butt welded Al alloys.-International Journal of Fatigue, 2005, 27, p.305-16.
16. **Colligan, J., Paul, J., Konkol., James, J., Fisher., Pickens Joseph, R.** Friction stir welding demonstrated for combat vehicle construction.-Welding Journal, 2002, p.1-6.

N. Shanmuga Sundaram, N. Murugan

TRINTIMI SUVIRINTO ALIUMINIO LYDINIO AA2024-T6 DIDŽIAUSIOS TEMPIMO STIPRUMO RIBOS PRIKLAUSOMYBĖ NUO SUVIRINIMO TRINTIMI TECHNOLOGINIO PROCESO PARAMETRŲ

R e z i u m ė

Aliuminio lydinys AA2024-T6 (Al–Cu lydinys) plačiai naudojamas labai stiprioms konstrukcijoms gaminti, taip pat aviacijos pramonėje, kur reikalingas didelis medžiagą veikiančių jėgų ir jos svorio santykis ir didelis plastiškumas. Dėl blogo suvirinamumo, lydomasis suvirinimas dažniausiai netinka 2xxx ir 7xxx serijos aliuminio lydiniams. Suvirinamas trintimi – tai technologinis procesas, kurio metu nepasiekiama medžiagos lydymosi temperatūra. Jis tinka minėto tipo lydiniams sujungti. Suvirinimo parametrai: suvirinimo greitis, įrankio sukimosi greitis, jo antgalio skersmuo, profilis bei veikianti ašinė jėga, turi įtakos suvirinimo trintimi siūlės mechaninėms savybėms. Sudarytas matematinis modelis, leidžiantis numatyti trintimi suvirinto aliuminio lydinio AA2024-T6 didžiausią tempimo stiprumo ribą. Eksperimentui atlikti taikytas statistinis Box-Behnken eksperimentinio planavimo metodas. Modeliui sudaryti taikytas paviršiaus reakcijos į apkrovas metodas. Sudarytas modelis patikrintas naudojant statistinės analizės variacijų programinę įrangą (ANOVA). Detaliai išanalizuota anksčiau paminėtų technologinio proceso parametrų įtaka trintimi suvirintų siūlių elgsenai tempiant.

N. Shanmuga Sundaram, N. Murugan

DEPENDENCE OF ULTIMATE TENSILE STRENGTH OF FRICTION STIR WELDED AA2024-T6 ALUMINIUM ALLOY ON FRICTION STIR WELDING PROCESS PARAMETERS

S u m m a r y

The aluminium alloy AA2024-T6 (Al–Cu alloy) has been widely used in the fabrication of high strength structures and in aircraft industries requiring a high strength-to-weight ratio and good ductility. Normally fusion welding processes are not suitable for welding of 2xxx and 7xxx series aluminium alloys due to their poor weldability. On the other hand Friction Stir Welding (FSW) process is an emerging solid joining process especially suitable for joining of such alloys. The welding parameters such as tool rotational speed, welding speed, tool pin diameter, axial force and tool pin profile significantly influence the mechanical properties of the FS welded joint. Mathematical model to predict the ultimate tensile strength (UTS) of the friction stir welded AA2024-T6 aluminium alloy were developed. Box-Behnken design was used to conduct the experiments and response surface method (RSM) was employed to develop the model. The developed model was validated using the statistical tool analysis of variance (ANOVA). The interaction effects of the above process parameters on tensile behaviour of the friction welded joints are discussed in detail.

Н. Шанмуга Сундарам, Н. Муруган

ЗАВИСИМОСТЬ ПРЕДЕЛА ПРОЧНОСТИ ПРИ РАСТЯЖЕНИИ АЛЮМИНИЕВОГО СПЛАВА AA2024-T6, СВАРЕННОГО ТРЕНИЕМ ОТ ПАРАМЕТРОВ ТЕХНОЛОГИЧЕСКОГО ПРОЦЕССА

Р е з ю м е

Алюминиевый сплав AA2024-T6 (сплав Al-Cu) широко используется при изготовлении конструкций высокой прочности и в авиационной промышленности, где требуется высокое соотношение между воздействующими на конструкцию силами и ее весом и высокая пластичность. Из-за плохой свариваемости, сварка плавлением неприменима алюминиевым сплавам 2xxx и 7xxx серии. Сварка трением – это технологический процесс, при котором процесс соединения деталей происходит, не достигая температуры плавления их материала. Это применимо для соединения сплава выше упомянутого типа. Параметры сварки: скорость сварки, скорость вращения инструмента, диаметр его наконечника и профиль, осевая сила, действующая на инструмент, влияет на механические свойства шва, сваренного трением. Предложена математическая модель, позволяющая определить наивысший предел прочности при растяжении алюминиевого сплава AA2024-T6, сваренного трением. Для проведения экспериментальных исследований использован статистический метод экспериментального планирования Вох-Вегнкен. Для создания модели использован метод поверхностной реакции на нагрузку. Созданная модель, проверена с помощью программного оборудования предназначенного для проведения статистического анализа вариаций (ANOVA). Детально проанализировано влияние вышеупомянутых параметров технологического процесса на поведение швов, сваренных трением.

Received June 19, 2009
Accepted August 07, 2009